ELSEVIER

Biochemical Pharmacology 65 (2003) 25–34

Biochemical Pharmacology

Plasma stability of two glycosyl indolocarbazole antitumor agents

Jean-François Goossens[a], Jérôme Kluza[b], Hervé Vezin[c], Mustapha Kouach[d], Gilbert Briand[d], Brigitte Baldeyrou[b], Nicole Wattez[b], Christian Bailly[b,*]

[a]*Laboratoire de Chimie Analytique, Faculté des Sciences Pharmaceutiques et Biologiques, Université de Lille 2, 59006 Lille, France*
[b]*Laboratoire de Pharmacologie Antitumorale du Centre Oscar Lambret—INSERM U-524, IRCL, Place de Verdun, 59045 Lille, France*
[c]*Laboratoire de Chimie Organique Physique, URA CNRS 351, USTL Bât. C3, 59655 Villeneuve d'Ascq, France*
[d]*Laboratoire de Spectrométrie de Masse, Université de Lille II, 59045 Lille, France*

Received 4 July 2002; accepted 28 August 2002

Abstract

In recent years, several glycosyl indolocarbazole derivatives have been developed as antitumor agents targeting the topoisomerase I-DNA complex and a few of them were evaluated in clinical trials. The lead drug in the series is compound **A** which bears a formylamino substituent on the *N*-imide F-ring. This compound has shown promising antitumor activities *in vivo* and was tested clinically but it has been recently replaced with a more active analogue, J-107088, bearing a (hydroxymethyl-2-hydroxy) ethylamino substituent on the *N*-imide F-ring. We have compared the plasma stability of two molecules in this series, compounds **A** and **D**, which only differ by the nature of the group on the imide ring. The conversion of the compounds into the anhydride species **B** was studied by HPLC and the resulting metabolite, formed both in human plasma ultrafiltrate and in water, was characterized by NMR and mass spectrometry. Absorption measurements provided a facile method to follow the conversion of compounds **A** and **D** into their metabolite product **B**. Altogether, the experimental data demonstrate that the replacement of the NHCHO substituent of compound **A** with a hydrophilic $NHCH(CH_2OH)_2$ chain preserves the intact imide function that is known to be essential for topoisomerase I inhibition and cytotoxicity. The transformation of compound **A** into the anhydride metabolite **B** (or its diacid open form) occurs much more slowly compared to compound **D**. Half-life parameter $t_{1/2}$ of 67 and 245 min^{-1} were calculated for compounds **A** and **D**, respectively. A molecular modeling analysis, performed to compare the conformation and electronic properties of compounds **A** and **D**, offers a rational explanation for the gain of chemical stability of the indolocarbazole derivative **D**. The data provide important information for the rational design of antitumor indolocarbazole derivatives.

Keywords: Indolocarbazole; Plasma stability; Antitumor drug; Carbohydrate; Rebeccamycin

1. Introduction

The indolocarbazole antibiotics BE13793C, AT2433-B1 and rebeccamycin (Fig. 1) have provided lead structures for the development of antitumor drugs targeted to DNA topoisomerase I [1,2]. The chief compound in the series is the glycosyl derivative **A** (Fig. 2) which intercalates into DNA and potently inhibits topoisomerase I [3–5]. This synthetic compound has shown remarkable antitumor activities *in vitro* and in animal models [6,7] and was then advanced to clinical trials [8,9].

A significant number of derivatives of rebeccamycin and compound **A** have been synthesized over the past 10 years [10]. In the course of a structure-activity relationship program at Banyu Pharmaceuticals (Japan), the analogue J-107088 was synthesized and tested [11]. This newly designed compound was shown to exhibit superior antitumor activity to compound **A** [12–14]. Molecular studies in our laboratories have provided useful information that account, at least partially, for this enhanced activity. The relocation of the two OH groups from the 1,11 positions to the 2,10 positions strongly reduces the ability of the compound to intercalate into DNA while preserving the anti-topoisomerase I activity [15]. The other modification on the maleimide F-ring also has a significant effect on the mechanism of action of the compound. The substitution of the (hydroxymethyl-2-hydroxy)ethylamino for the formylamino group of compound **A** increases DNA affinity by a factor of four but does not affect topoisomerase I inhibition [16]. Both the NHCHO → $NHCH(CH_2OH)_2$ substitution and the relocation of the two OH groups increase the

* Corresponding author. Tel.: +33-320-169-218; fax: +33-320-169-229.
E-mail address: bailly@lille.inserm.fr (C. Bailly).

0006-2952/02/$ – see front matter
PII: S0006-2952(02)01418-1

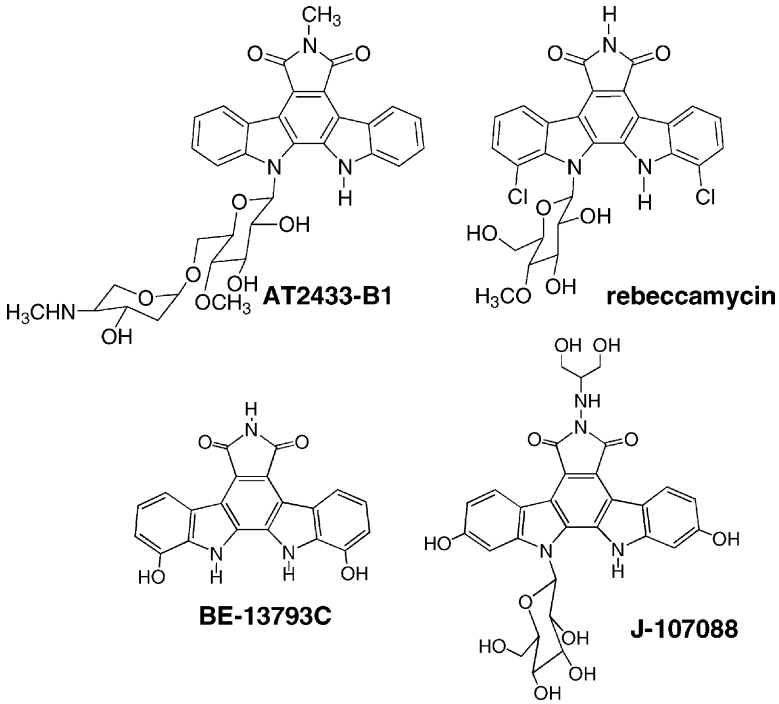

Fig. 1. Four antitumor indolocarbazoles.

cytotoxic potential of compound **A** by a factor of about 4 and 10, respectively [15,16].

The metabolism of compound **A** has been studied both *in vitro* and *in vivo*, in animals and in humans [17,18]. In rodent plasma, the drug is primarily converted to its deformyl derivative **C** whereas in dog and human plasma, the metabolization essentially provides the deformylhydrazine form of **A**. The resulting anhydride metabolite **B** is inactive. It has been suggested that the conversion of **A** into **B** is catalyzed by metal ions. The potential formation of a compound **A**:M^{n+} complex would catalyze the opening of the maleimide F-ring, as depicted in Fig. 2b [18].

In this study, we have compared the water and plasma stability of compounds **A** and **D** which only differ by the

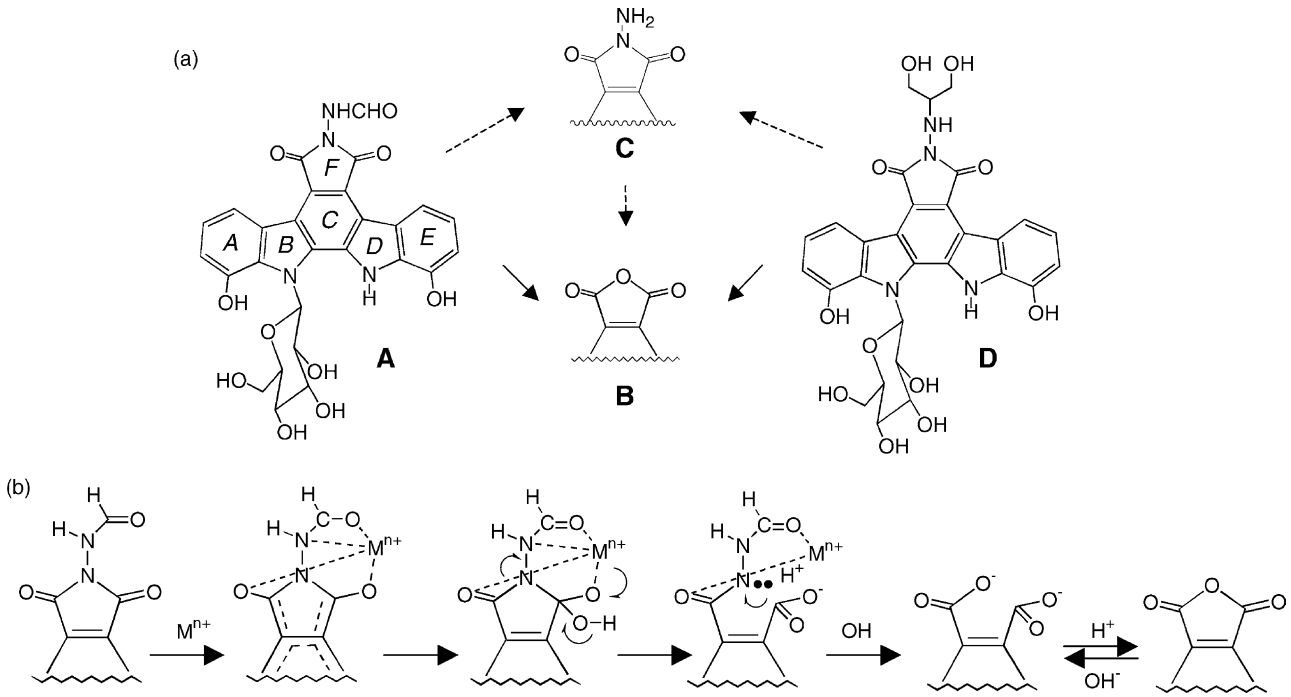

Fig. 2. (a) Structures of the two drugs **A** and **D** used in this study and their metabolites **B** and **C**. (b) Metal-dependent pathway proposed for the transformation of compound **A** into its anhydride metabolite (adapted from [18]).

F-ring substituent (Fig. 2a). The anhydride metabolite formed in plasma and water was characterized by NMR and mass spectrometry. HPLC analysis clearly shows that the incorporation of the (hydroxymethyl-2-hydroxy)ethylamino substituent in place of the formylamino group of **A** significantly reduces the rate of metabolization of the compound into the inactive anhydride form. This important experimental result, complemented by a molecular modeling analysis, provides a sound molecular basis to explain the enhanced cytotoxicity of **D** and J-107088 compared to compound **A**.

2. Materials and methods

2.1. Drugs

The two indolocarbazole drugs were kindly provided by Dr T. Yoshinari and Dr H. Arakawa (Banyu Pharmaceuticals Co., Ltd.). Their chemical synthesis has been reported [11,19]. The drugs were first dissolved in dimethylsulfoxide (DMSO) at 10 mM and then further diluted with water. The stock solutions of drugs were kept at −20° and freshly diluted to the desired concentration immediately prior to use. All other chemicals were analytical grade reagents.

2.2. Absorption spectra

Spectra were recorded using an Uvikon 943 spectrophotometer coupled to a Neslab RTE111 cryostat. For each series of measurements, 12 samples were placed in a thermostatically controlled cell-holder, and the quartz cuvettes (10 mm pathlength) were heated by circulating water. The temperature inside the cuvette was measured with a platinum probe.

2.3. Samples preparation

Compounds **A** and **D** at a final concentration of 10 μg/mL were incubated with plasma ultrafiltrate. To obtain 200 μL of ultrafiltrate, 1 mL of human plasma was centrifugated at 2080 *g* for 30 min using a Centrifree Millipore tube (Amicon bioseparation) which retains high molecular weight plasma proteins. After an incubation period varying from 0 to 120 min, a 800 μL aliquot of each sample was purified by solid/liquid extraction. Briefly, the sample is loaded onto a C_{18} SEP-PAK® cartridge (Millipore) preconditioned by addition of methanol, water and 0.02 M glycine buffer, pH 2.8, successively. After loading the sample, the cartridge is washed successively with one volume of H_2O and MeOH/H_2O 1:9 and elution is performed by addition of 1 mL EtOH. The eluent is evaporated to dryness and the residue is reconstituted in 200 μL of the chromatographic mobile phase indicated below. A 20 μL aliquot is then analyzed by high performance chromatography.

2.4. HPLC equipment

Analytical chromatography was carried out on Chromsep column (C_{18}, 150 × 4.6 mm i.d., 5 μm particle size, Chrompack France). A guard column (10 × 3 mm i.d., 5 μm particle size) with the same stationary phase was used. A constant mobile phase flow of 0.7 mL/min was provided by a Beckman metering pump model (Beckman Coulter) equipped with a Rheodyne injector (20 μL loop). Isocratic elutions using acetonitrile/methanol/water mixture 18:23:59 acidified with H_3PO_4 at pH 2.7 were performed at 25°. The absorption spectrum of the column eluate was recorded from 210 to 600 nm (λ_{max} = 305 nm) using a Beckman photodiode array spectrophotometer. Chromatographic data were collected and processed on a digital computer running with the Beckman software.

2.5. NMR and ion-spray mass spectrometry

^{1}H NMR spectra were recorded on a Bruker AC 300 spectrometer. 512 Data points were accumulated for each spectrum using a pre-saturation sequence to suppress the water peak solvent. Chemical shifts were attributed with reference to the known NMR spectrum of **A** [19] and using also the calculated NMR data for this compound. For ion-spray mass spectrometry, samples were prepared in a solution containing 50% acetonitrile and 1% triethanolamine in water, and the samples injected in a simple-quadrupole mass spectrometer API I (Perkin–Elmer Sciex) equipped with an ion-spray (nebulizer-assisted electrospray) source (Sciex). The solutions were continuously infused with a medical infusion pump (Model 11, Harvard Apparatus) at a flow rate of 5 μL/min. Polypropylene glycol (PPG) was used to calibrate the quadrupole. Ion-spray mass spectra were acquired at unit resolution by scanning from *m/z* 300 to 700 with a step size of 0.1 Da and a dwell time of 2 ms. Ten spectra were summed and recorded at an orifice voltage of −60 V whereas the potential of spray needle was held at −4.5 kV.

2.6. Computational chemistry

All calculations were performed on a NT workstation (PIII-650 MHz processor) using the Spartan Pro V 1.0.1 software package. A conformational analysis was performed for compounds **A** and **D** on all rotatable bonds using the Monte Carlo procedure implemented in Spartan. The resulting structures were minimized using a MMF94 force field and fully optimized at the *ab initio* RHF/3-21G* level. Hydration energies were calculated using the RHF/PM3-SM5.4 method. The log values of octanol/water partition coefficients (log *P*) were calculated using the Villar method with a semi-empirical function implemented in Spartan [20,21].

3. Results

3.1. Plasma stability

The two indolocarbazole derivatives **A** and **D**, which only differ by the nature of the substituent on the maleimide nitrogen (Fig. 2a), were incubated in plasma ultrafiltrate at 37° for up to 3.5 hr and the resulting solution was analyzed by absorption spectroscopy and liquid chromatography. The absorption measurements are presented in Fig. 3. Similar spectral changes were observed with **A** and **D**. In both cases, the absorption band of the parent compound centered at 315 nm gradually decreases and a new band is formed at 280 nm. The presence of well resolved isosbestic points suggests that the starting material is directly transformed into a second species; the metabolic transformation is homogeneous. The important shift of the main band to a lower wavelength (blue shift) indicates that the aromaticity of the indolocarbazole is significantly changed and this is consistent with the expected opening of the maleimide ring. At this point, it can already be seen that the spectral changes are less pronounced with **D** compared to **A** suggesting that the former compound is more stable than the latter. HPLC analyses, performed with an absorbance detection at 305 nm, fully confirm this observation.

A set of typical chromatograms obtained with **A** is presented in Fig. 4. Under our experimental conditions, a well resolved peak eluting at 808.8 ± 11.3 s (13.50± 0.19 min) is detected with **A** at t_0, i.e. immediately after the addition of the drug to the plasma solution. With time, this peak gradually decreases and a second sharp peak appears at 460.0 ± 4.4 s (7.67 ± 0.07 min). Similar profiles were obtained with **D**. In this case, the unmodified compound **D** eluted at 859.4 ± 12.4 s (14.32 ± 0.21 min) and the retention time was 459.6 ± 5.4 s (7.66 ± 0.09 min) for its metabolite. The two metabolites obtained with **A** and **D** showed identical retention times and their absorption spectra were also identical with a maximum centered at 280 nm. The absorption and HPLC measurements suggest that the two compounds are converted to the same metabolite, most likely the hydrolyzed form (i.e. the diacid) of the anhydride metabolite **B**.

A kinetic analysis of the metabolization process gave the curve shown in Fig. 5a. The area under each HPLC peak for

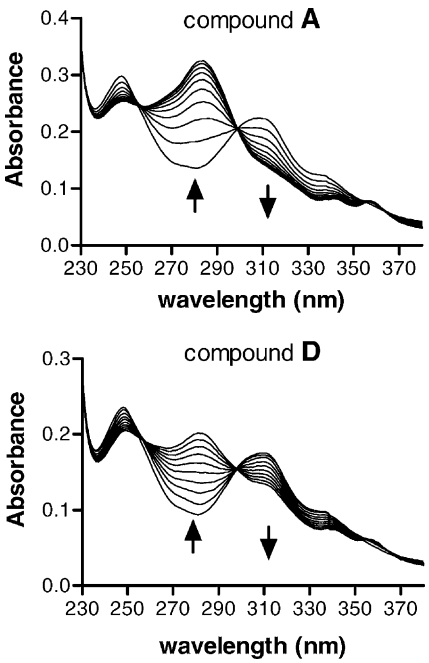

Fig. 3. Absorption spectra of a solution of **A** and **D** (10 mg/mL) incubated at 37° in human plasma ultrafiltrate. The spectra were recorded at intervals every 20 min for 200 min in a total volume of 80 mL.

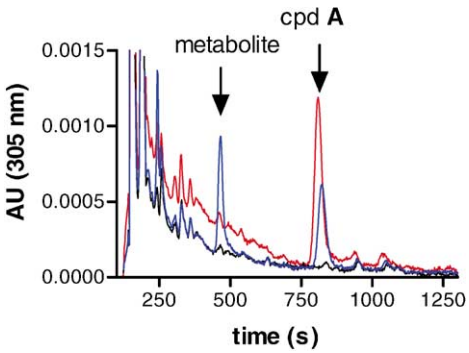

Fig. 4. Typical HPLC profiles of compound **A** in plasma ultrafiltrate. The red and blue profiles refer to the solution of **A** at $t = 0$ (immediately after addition to the plasma) and $t = 200$ min, respectively. The black line corresponds to the injection of plasma alone. The samples were analyzed using an isocratic mobile phase with detection by absorption at 305 nm. Flow rate 0.7 mL/min.

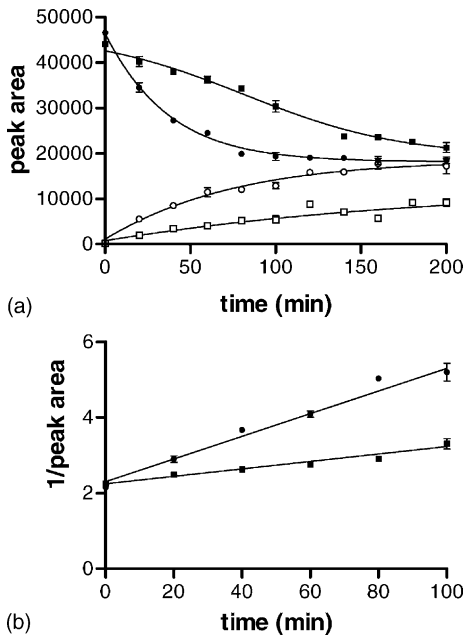

Fig. 5. (a) Metabolism of **A** and **D** in human plasma ultrafiltrate at 37°. The graph shows the decrease of (●) **A** and (■) **D**, with the corresponding increase of the metabolite for (○) **A** and (□) **D**. (b) Representations of a two order rate reaction. Each value represents the mean of three independent experiments performed in duplicate.

the starting material and the transformed species was calculated as a function of time. The decrease of the peak area is significantly more rapid for **A** compared to **D**. For example, after 40 min incubation in the plasma, the peak of **A** was reduced by 42% whereas that of **D** was reduced by only 14%. After 80 min, we recovered 42% of **A** and 78% of **D**. The latter compound is thus much more stable in the plasma than the parent drug. In other words, the substitution of a (hydroxymethyl-2-hydroxy)ethylamino substituent for the formylamino group of **A** greatly reinforces the stability of the drug in the plasma. A more direct view of the enhanced stability of **D** compared to **A** is provided by the graph shown in Fig. 5b in which the inverse of the area under peak is plotted as a function of time. Linear regressions for **A** and **D** ($r = 0.98$ and $r = 0.99$, respectively) suggested a two order rate reaction. From this representation, we calculated the half-life parameter $t_{1/2}$: 67 and 245 min^{-1} for **A** and **D**, respectively. Therefore, the data indicate that the replacement of the NHCHO substituent of **A** by the $NHCH(CH_2OH)_2$ functionality in **D** increases the plasma stability of the molecule by a factor of 3.6. The anhydride **B** represents the common metabolite of **A** and **D**. This compound has been previously identified both *in vitro* and *in vivo* in the study of the metabolism of **A** [17,18].

3.2. NMR and MS characterization of the metabolite *B*

A 2-mL solution of **A** at 1 mg/mL in water was split in two tubes. The first one was heated from 20 to 80° at a rate of 1°/min and the absorption spectrum of the solution was recorded every 6 min (10 cycles). After the 10th cycle, the solution at 80° was cooled to room temperature, lyophilized and the resulting material was then dissolved in 500 mL of a deuterated water:DMSO mixture (1:1) for

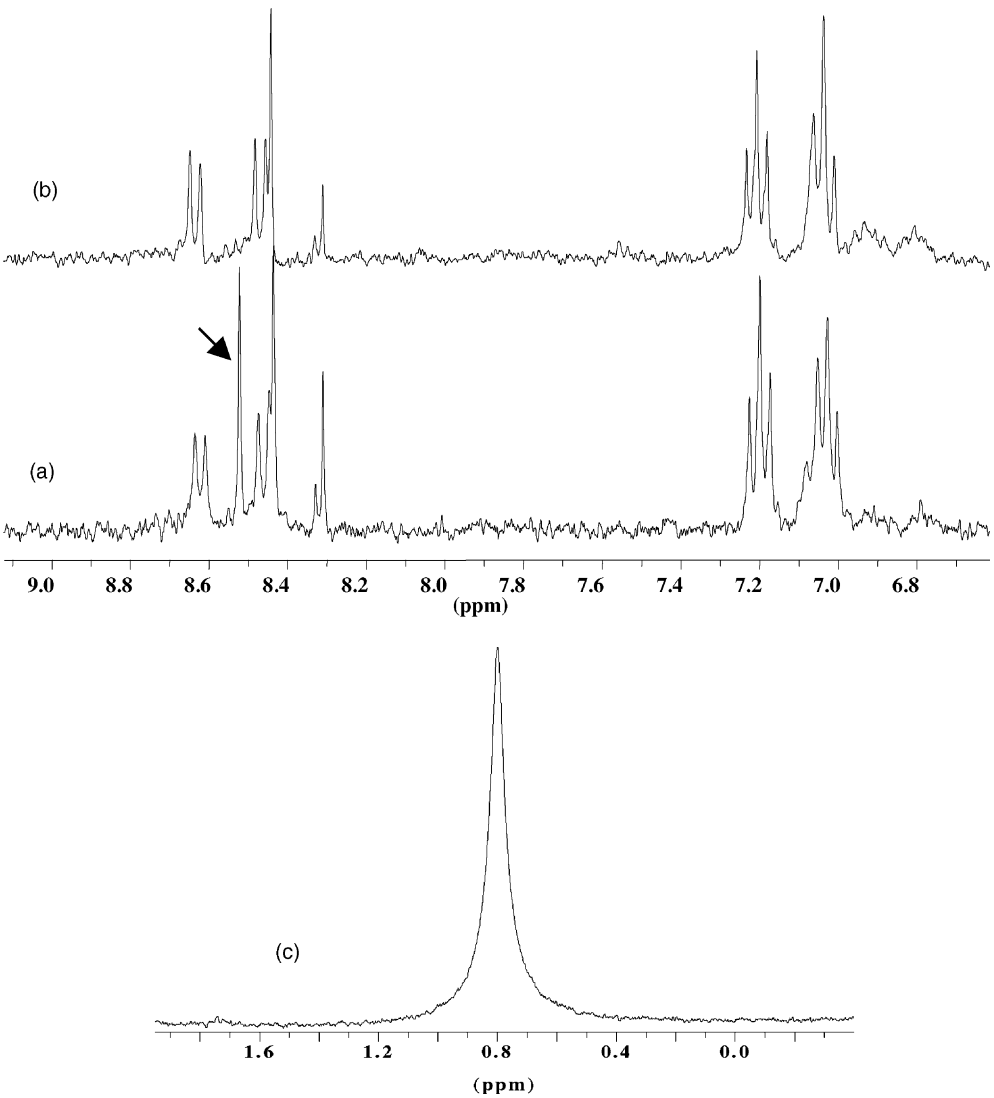

Fig. 6. ^{1}H NMR spectra of a solution of compound **A** (a) maintained at room temperature or (b) heated from 20 to 80° over 1 hr (1°/min). Only the region corresponding to the aromatic protons is shown. Panel (c) shows a portion of the ^{1}H NMR spectrum of the heated solution (same as in b) corresponding to the high field 0–2 ppm region showing the peak of hydrazine at 0.8 ppm. The initial drug solution was made in water at 1 mg/mL, heated or not, lyophilized and then the material was redissolved in 500 μL of a deuterated water:DMSO mixture (1:1).

the NMR analysis. The second tube was not heated but incubated for 1 hr at room temperature and then treated the same way as the other half of the initial solution. The absorption measurements were consistent with those presented in Fig. 3. The absorption spectrum of the 'cold' (non-heated) solution showed a band centered at 310 nm whereas the heated solution was characterized by a band at 280 nm. The pronounced blue shift reflects the opening of the maleimide ring. The solutions were then analyzed by proton NMR and the aromatic regions of the spectra are presented in Fig. 6. The aromatic protons show little or no modification upon heating of the solution of compound **A** indicating that the indolocarbazole ring system is not affected. In sharp contrast, the aldehyde proton frequency at 8.52 ppm disappears completely (compare spectra (a) and (b) in Fig. 6), indicating therefore that the heating of the solution results in the hydrolysis of the aldehyde function. Simultaneously, a new broad peak of 18 Hz appears at a chemical shift of 0.8 ppm (spectrum (c) in Fig. 6) and corresponds to the concomitant production of hydrazine (NH_2–NH_2). These observations reflect the conversion of **A** in the anhydride or more likely the corresponding diacid form. The protons of the two acid functions were not identified due to rapid exchange with water.

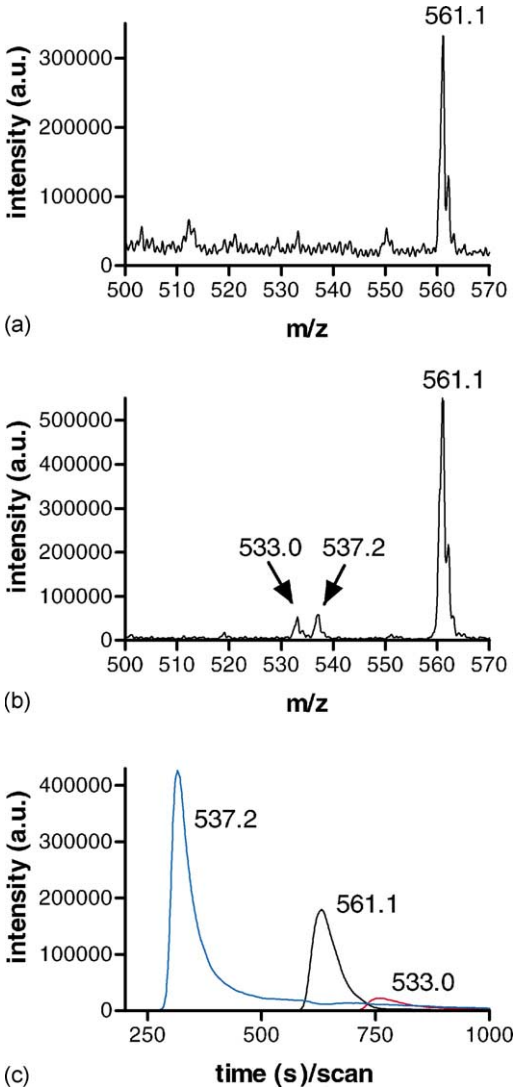

Fig. 7. Electrospray ionization mass spectra of compound **A** (a) before and (b) after heating up to 80° in water for 2 hr (negative ion mode). The peaks at $m/z = 561.1$, 537.2 and 533 correspond to compounds **A**, **B** (in the open diacid form) and **C**, respectively. Panel (c) shows the selected ion monitoring (SIM) detection of the different species (see text for details).

The heat-induced transformation of **A** was also followed my mass spectrometry. The mass spectrum of a solution of compound **A** shows a well resolved peak at $m/z = 561.1$ $(M - H)^-$ (Fig. 7a). The heating of the solution results in the formation of a peak at $m/z = 537.2$ which is the expected mass for the diacid (Fig. 7b). In addition, we could also detect a peak at $m/z = 533$ which we reasonably attribute to the amino compound **C**. It may correspond to the intermediate species formed after hydrolysis of the formaldehyde group of **A** and prior to eliminating the hydrazine function to generate the diacid or the anhydride. This peak at $m/z = 533$ always remains very small and represents only a few % of the total material (even after the full heating process) whereas the peak at $m/z = 537.2$ increases considerably. For example, the mass spectrometry analysis under the selected ion monitoring (SIM) detection (Fig. 7c) indicates that a solution of **A** at 10 μg/mL in water heated for 7 days at 65° contains 3.5% compound **C** ($m/z = 533$), 67.9% compound **B** ($m/z = 537.2$) and 28.6% compound **A** ($m/z = 561.1$). Altogether, the NMR and mass spectrometry data are fully consistent with the heat-induced transformation of A into its diacid metabolite, i.e. the open form of the anhydride B identified in human plasma [18].

The above physicochemical data establish that in water compound **A** hydrolyzes to give compound **B**. HPLC analyses showed that this is the same metabolite as the one formed in human plasma. When a water solution of compound **A** heated to 95° for 1 hr was mixed with

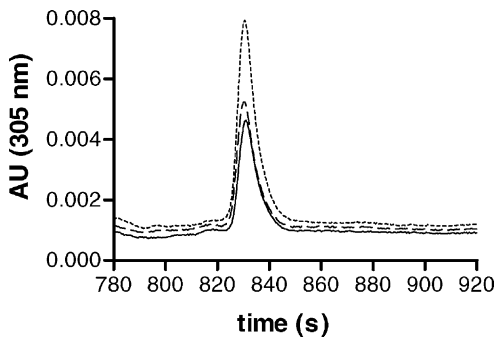

Fig. 8. Identical HPLC profiles for the metabolite of compound **A** formed in plasma ultrafiltrate and in water. A sample of compound **A** in plasma ultrafiltrate maintained at 37° for 6 hr (thick solid line) was mixed with a solution of compound **A** heated to 95° for 1 hr (dashed line). In both cases, the metabolite thus formed eluted at the same time (dotted line) and presented the exactly the same absorption spectrum recorded with a diode array. The samples were analyzed using an isocratic mobile phase with detection by absorption at 305 nm. Flow rate 0.5 mL/min.

Table 1
Calculated physicochemical properties

Compounds	Surface (Å^2)	Volume (Å^3)	Dipole (Debye)	Log P	ΔH_{hydra} (kcal/mol)	E_{HOMO} (eV)	E_{LUMO} (eV)
A	522.4	555	8.08	−1.28 (±0.6)	−26.1	−8.41	−1.36
D	561	603	8.38	−5.75 (±0.9)	−63.3	−7.18	+1.13

increasing volumes of the solution of compound **A** incubated in plasma ultrafiltrate at 37°, the metabolite separated by HPLC had the same retention time (Fig. 8) and the compound thus separated showed an absorption spectrum characteristic of the modified F-ring with a maximum at 280 nm (data not shown). A prolonged incubation of compound **A** in human plasma at 37° gives the same metabolite as the heated solution of compound **A** in water.

3.3. Conformational and molecular orbital analyses

The conformational analysis revealed significant differences between the two indolocarbazole compounds. Not only the surfaces, molecular volumes and hydrophobicity of the two molecules are different (Table 1) but also the orientation of the carbohydrate residue differs significantly. According to the calculated Log P values, compound **A** exhibits a much higher hydrophobicity than its analogue **D**. The calculated solvation energies (ΔH_{hydra}) indicate that **A** is 2–3 times less hydrated than **D** (Table 1). The marked differences between the two drugs in terms of hydrophobicity and solvation energies may account, at least partially, for their different plasma stabilities.

From the molecular orbital analysis, another interesting consideration is the distribution of the energies of the highest occupied molecular orbital (E_{HOMO}) and lowest unoccupied molecular orbital (E_{LUMO}) along the molecules, as calculated by quantum mechanical methods at the

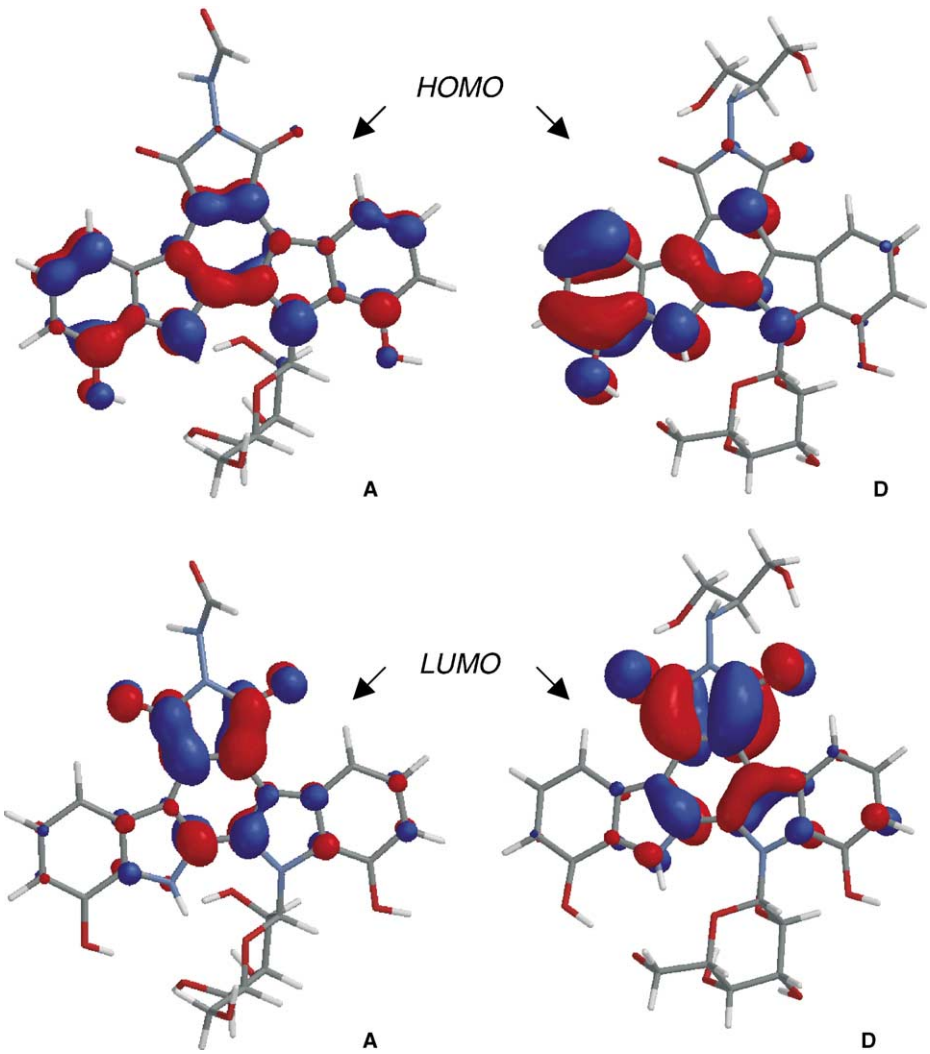

Fig. 9. HOMO and LUMO distribution for the most stable calculated configurations **A** and **D**.

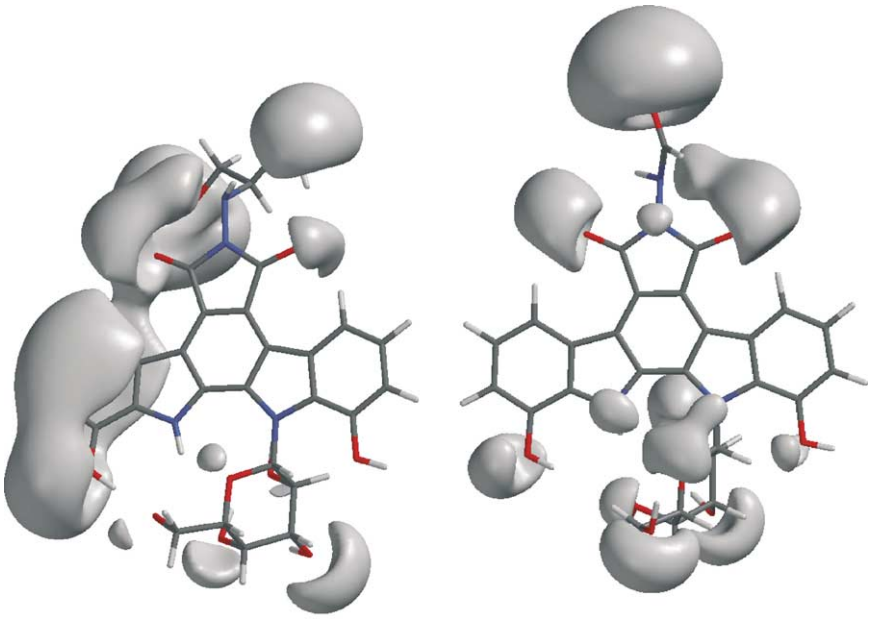

Fig. 10. Electrostatic potential map for **A** and **D**.

ab initio 3-21G* level (Fig. 9). The distribution of the HOMO and LUMO energies is quite different for the two molecules but however in both cases the HOMO density is high on the free NH indole nitrogen indicating a strong nucleophilic reactivity. This indole NH group, which likely serves as an electron-withdrawing group, is a key element for the DNA interaction. For **D**, the HOMO energy is essentially localized on the indole ring which is not linked to the carbohydrate residue. This side of the molecule also carries most of the electrostatic potential, as indicated by the map shown in Fig. 10. This is probably the side involved in the interaction between the drug and electron poor regions of the DNA-topoisomerase I complex. The LUMO energy is considerably distinct for the two compounds. The 2 eV difference suggests that the electrophilic reactivity is much higher for **A** compared to **D** and this observation is very likely to account for the higher plasma stability of **D** compared to **A**. To sum up, the molecular orbital analysis reveals that the band gap energy $\Delta\varepsilon$ ($\Delta\varepsilon = E_{HOMO} - E_{LUMO}$) is lower for **D** ($\Delta\varepsilon = -8.31$ eV) compared to **A** ($\Delta\varepsilon = -7.05$ eV) and this can explain the lower chemical reactivity of the new analogue. Therefore, the computational data are fully compatible with the experimental results and provide a sound molecular basis to explain the gain of stability obtained by replacing the NHCHO substituent on the nitrogen imide of **A** by a more polar $NHCH(CH_2OH)_2$ group.

4. Discussion

Until recently, compound **A** was the only topoisomerase I-targeted indolocarbazole tested clinically. The potent inhibition of the DNA cleavage and the kinase activities of topoisomerase I by this compound is responsible for the high cytotoxic potential against different tumor cell lines [22,23]. In animal models, compound **A** was found to be highly potent against different experimental tumors [3,5]. For example, the drug caused significant regression of nodules of human PC-13 lung cancer and MKN-45 stomach cancer cells and showed a lower cumulative toxicity than conventional anticancer drugs like etoposide and cisplatinum [5]. The potent anticancer effects in transplanted tumors in mice coupled with its low cumulative toxicity have justified the setting of clinical trials with this drug [8,9]. But later, the clinical trials with compound **A** were interrupted due to insufficient responses. However, further drug design in this series leads to the development of a new anticancer drug candidate structurally close to compound **A**: the drug J-107088 (Fig. 1).

In the course of their structure-activity relationship studies, chemists at the Banyu Tsukuba Research Institute (Japan) identified the compound J-107388 as a highly potent topoisomerase I poison [12]. This new compound differs from compound **A** by two aspects. First, the two hydroxyl groups on the IND chromophore have been shifted from positions 1,11 to positions 2,10. We have shown previously that the relocation of the OH groups considerably reduces the capacity of the drug to bind to DNA but affects neither its capacity to stabilize topoisomerase I-DNA complexes, nor to inhibit the SR protein kinase activity of the enzyme [22,24]. Second, the formylamino substituent on the imide F-ring nitrogen, supposed to establish a direct contact with topoisomerase I [15], has been replaced with a more polar $NHCH(CH_2OH)_2$ group. This chain, positively charged at neutral pH, increases the aqueous solubility of the molecule

and reinforces its DNA binding interaction without penalizing the action on topoisomerase I [16]. But importantly, we demonstrate here that the newly introduced substituent contributes to limit the hydrolysis of the compound into its inactive anhydride form, referred to as compound **B**. A metal-dependent catabolic pathway has been postulated to explain the conversion of compound **A** into its deformylated amino product and then its anhydride derivative [17,18]. Our data indicate that in human plasma, the transformation of compound **A** into the metabolite **B** occurs much more slowly compared to compound **D** (Fig. 5). Capping the nitrogen F-ring with a $NHCH(CH_2OH)_2$ chain preserves the intact imide function that is essential for topoisomerase I inhibition. J-107088 which combines the two types of structural changes has shown remarkable antitumor activities *in vivo* on murine and human tumors transplanted in mice and it was found to be active in a much wider range than compound **A** [13,14].

The work reported here provides key information on the factors that govern the plasma stability of glycosyl indolocarbazole derivatives. The $NHCH(CH_2OH)_2$ substituent introduced on the F-ring of the indolocarbazole serves as a protecting group to maintain the imide function as well as it plays a role in the interaction with the molecular targets, DNA and topoisomerase I [16]. We have quantified the transformation of compounds **A** and **D** into the anhydride metabolite **B** (or the equivalent open diacid form) by HPLC and the resulting species was characterized by NMR and mass spectrometry. A complementary interesting observation is that the same metabolite is formed both in the human plasma ultrafiltrate and in water, permitting thus a facile identification of the chemical stability of the molecules. The simple UV measurements, coupled to mass spectrometry, will be of general interest to compare the intrinsic stability of a variety of glycosyl indolocarbazole compounds. We are now in the process of evaluating by similar absorption measurements the chemical stability of the many analogues synthesized previously in the course of our extensive structure-activity relationships studies [25–27]. The molecular modeling information described here greatly help to rationally design analogues with a further increased plasma stability.

Acknowledgments

This work was done under the support of research grants (to C.B.) from the Ligue Nationale Française Contre le Cancer (Equipe Labellisée LA LIGUE).

References

[1] Bailly C. Topoisomerase I poisons and suppressors as anticancer drugs. Current Med Chem 2000;7:39–58.

[2] Long BH, Balasubramanian BN. Non-camptothecin topoisomerase I compounds as potential anticancer agents. Exp Opin Ther Patents 2000;10:635–66.

[3] Yoshinari T, Matsumoto M, Arakawa H, Okada H, Noguchi K, Suda H, Okura A, Nishimura S. Novel antitumor indolocarbazole compound 6-*N*-formylamino-12,13-dihydro-1,11-dihydroxy-13-(β-D-glucopyranosyl)-5*H*-indolo[2,3-*a*]pyrrolo-[3,4-*c*]carbazole-5,7-(6*H*)-dione (NB-506): induction of topoisomerase I-mediated DNA cleavage and mechanisms of cell line-selective cytotoxicity. Cancer Res 1995;55:1310–5.

[4] Arakawa H, Matsumoto H, Morita M, Sasaki M, Taguchi K, Okura A, Nishimura S. Antimetastatic effect of a novel indolocarbazole (NB-506) on IMC-HM murine tumor cells metastasized to the liver. Jpn J Cancer Res 1996;87:518–23.

[5] Arakawa H, Iguchi T, Morita M, Yoshinari T, Kojiri K, Suda H, Okura A, Nishimura S. Novel indolocarbazole compound 6-*N*-formylamino-12,13-dihydro-1,11-dihydroxy-13-(β-D-glucopyranosyl)-5*H*-indolo-[2,3-*a*]pyrrolo-[3,4-*c*]carbazole-5,7-(6*H*)-dione (NB-506): its potent antitumor activities in mice. Cancer Res 1995;55:1316–20.

[6] Kanzawa F, Nishio K, Kubota N, Saijo N. Antitumor activities of a new indolocarbazole substance, NB-506, and establishment of NB-506-resistant cell lines, SBC-3/NB. Cancer Res 1995;55:2806–13.

[7] Vanhoefer U, Voigt W, Hilger RA, Yin MB, Harstrick A, Seeber S, Rustum YM. Cellular determinants of resistance to indolocarbazole analogue NB-506. A novel potent topoisomerase I inhibitor, in multidrug-resistant human tumor cells. Oncol Res 1997;9:485–94.

[8] Sasaki Y, Tanigawara Y, Fujii H, Ohtsu T, Wakita H, Igarashi T, Itoh K, Ogino H, Takenaga N, Okada K, Nishimura S, Abe K. Phase I and pharmacology study of NB-506. Proc Am Soc Clin Oncol 1995;14:172.

[9] Ohe Y, Tanigawara Y, Fujii H, Ohtsu T, Wakita H, Igarashi T, Minami H, Eguchi K, Shinkai T, Tamura T, Kunotoh H, Saijo N, Okada K, Ogino H, Sasaki Y. Phase I and pharmacology study of 5-day infusion of NB-506. Proc Am Soc Clin Oncol 1997;16:199a.

[10] Bailly C. Targeting DNA and topoisomerase I with indolocarbazole antitumor agents. In: Demeunynck M, Bailly C, Wilson WD, editors. DNA and RNA Binders, From Small Molecules to Drugs. Wiley; 2002, in press.

[11] Ohkubo M, Kojiri K, Kondo H, Tanaka S, Kawamoto H, Nishimura T, Nishimura I, Yoshinari T, Arakawa H, Suda H, Morishima H, Nishimura S. Synthesis and biological activities of topoisomerase I inhibitors, 6-*N*-amino analogues of NB-506. Bioorg Med Chem Lett 1999;9:1219–24.

[12] Yoshinari T, Ohkubo M, Fukasawa K, Egashira S, Hara Y, Matsumoto M, Nakai K, Arakawa H, Morishima H, Nishimura S. Mode of action of a new indolocarbazole anticancer agent, J-107088, targeting topoisomerase I. Cancer Res 1999;59:4271–5.

[13] Arakawa H, Morita M, Kodera T, Okura A, Ohkubo M, Morishima H, Nishimura S. *In vivo* antitumor activity of a novel indolocarbazole compound, J-107088, on murine and human tumors transplanted into mice. Jpn J Cancer Res 1999;90:1163–70.

[14] Cavazos CM, Keir ST, Yoshinari T, Bigner DD, Friedman HS. Therapeutic activity of the topoisomerase I inhibitor J-107088 [6-*N*-(1-hydroxymethyla-2-hydroxyl)ethylamino-12,13-dihydro-13-(beta-D-glucopyranosyl)-5*H*-indolo[2,3-*a*]-pyrrolo[3,4-*c*]-carbazole-5,7(6H)-dione]] against pediatric and adult central nervous system tumor xenografts. Cancer Chemother Pharmacol 2001;48:250–4.

[15] Bailly C, Dassonneville L, Colson P, Houssier C, Fukasawa K, Nishimura S, Yoshinari T. Intercalation into DNA is not required for inhibition of topoisomerase I by indolocarbazole antitumor agents. Cancer Res 1999;59:2853–60.

[16] Bailly C, Qu X, Chaires JB, Colson P, Houssier C, Ohkubo M, Nishimura S, Yoshinari T. Substitution at the F-ring *N*-imide of the indolocarbazole antitumor drug NB-506 increases the cytotoxicity, DNA binding and topoisomerase I inhibition activities. J Med Chem 1999;42:2927–35.

[17] Takenaga N, Ishii M, Nakajima S, Hasegawa T, Iwasa R, Ishizaki H, Kamei T. *In vivo* metabolism of a new anticancer agent, 6-*N*-formylamino-12,13-dihydro-1,11-dihydroxy-13-(β-D-glucopyranosil)-5*H*-indolo [2,3-*a*]pyrrolo [3,4-*c*]carbazole-5,7(6H)-dione (NB-506) in rats and dogs: pharmacokinetics, isolation, identification, and quantification of metabolites. Drug Metab Dispos 1999;27: 205–12.

[18] Takenaga N, Hasegawa T, Ishii M, Ishizaki H, Hata S, Kamei T. *In vitro* metabolism of a new anticancer agent, 6-*N*-formylamino-12,13-dihydro-1,11-dihydroxy-13-(β-D-glucopyranosil)-5*H*-indolo[2,3-*a*]pyrrolo[3,4-*c*]carbazole-5,7(6H)-dione (NB-506), in mice, rats, dogs, and humans. Drug Metab Dispos 1999;27:213–20.

[19] Ohkubo M, Kawamoto H, Ohno T, Nakano M, Morishima H. Synthesis of NB-506, a new anticancer agent. Tetrahedron 1997;53:585–92.

[20] Halgren TA. Merk Molecular Force Field. III. Molecular geometries and vibrational frequencies for MMFF94. J Comput Chem 1996;17: 553–86.

[21] Halgren TA, Nachbar RB. Merk Molecular Force Field. IV. Conformational energies and geometries for MMFF94. J Comput Chem 1996;17:587–615.

[22] Pilch B, Allemand E, Facompré M, Bailly C, Riou JF, Soret J, Tazi J. Specific inhibition of SR splicing factors phosphorylation, spliceosome assembly and splicing by the antitumor drug NB506. Cancer Res 2001;61:6876–84.

[23] Urasaki Y, Laco G, Takebayashi Y, Bailly C, Kohlhagen G, Pommier Y. Use of camptothecin-resistant mammalian cell lines to evaluate the role of topoisomerase I in the antiproliferative activity of the indolocarbazole, NB-506, and its toposiomerase I binding site. Cancer Res 2001;61:504–8.

[24] Bailly C, Carrasco C, Hamy F, Vezin H, Prudhomme M, Saleem A, Rubin E. The camptothecin-resistant topoisomerase I mutant F361S is cross-resistant to antitumor rebeccamycin derivatives. A model for topoisomerase I inhibition by indolocarbazoles. Biochemistry 1999; 38:8605–11.

[25] Anizon F, Belin L, Moreau P, Sancelme M, Voldoire A, Prudhomme M, Ollier M, Sevère D, Riou JF, Bailly C, Fabbro D, Meyer T. Syntheses and biological activity (topoisomerases inhibition, antitumoral and antimicrobial properties) of rebeccamycin analogues bearing modified sugar moieties and substituted on the imide nitrogen with a methyl group. J Med Chem 1997;40:3456–65.

[26] Moreau P, Anizon F, Sancelme M, Prudhomme M, Bailly C, Ollier M, Sevère D, Riou JF, Fabbro D, Meyer T, Aubertin AM. Syntheses and biological activities of rebeccamycin analogues. Introduction of a halogenoacetyl substituent. J Med Chem 1999;42:584–92.

[27] Moreau P, Anizon F, Sancelme M, Prudhomme M, Bailly C, Carrasco C, Ollier M, Sevère D, Riou JF, Fabbro D, Meyer T, Aubertin AM. Syntheses and biological evaluation of indolocarbazoles, analogues of rebeccamycin, modified at the imide heterocycle. J Med Chem 1998;41:1631–40.